The CRISPR Journal
Volume 6, Number 1, 2023

DOI: 10.1089/crispr.2022.0045

The CRISPR Journal

ORIGINAL RESEARCH

Gene Editing Corrects *In Vitro* a G > A *GLB1* Transition from a GM1 Gangliosidosis Patient

Delphine Leclerc,[1] Louise Goujon,[2] Sylvie Jaillard,[3,4] Bénédicte Nouyou,[4] Laurence Cluzeau,[4] Léna Damaj,[5] Christèle Dubourg,[6,7] Amandine Etcheverry,[6] Thierry Levade,[8] Roseline Froissart,[9] Stéphane Dréano,[7] Xavier Guillory,[1,10] Leif A Eriksson,[11] Erika Launay,[4] Frédéric Mouriaux,[1,12] Marc-Antoine Belaud-Rotureau,[3,4] Sylvie Odent,[2,7] and David Gilot[1,4,*]

Abstract

Ganglioside-monosialic acid (GM1) gangliosidosis, a rare autosomal recessive disorder, is frequently caused by deleterious single nucleotide variants (SNVs) in *GLB1* gene. These variants result in reduced β-galactosidase (β-gal) activity, leading to neurodegeneration associated with premature death. Currently, no effective therapy for GM1 gangliosidosis is available. Three ongoing clinical trials aim to deliver a functional copy of the *GLB1* gene to stop disease progression. In this study, we show that 41% of *GLB1* pathogenic SNVs can be replaced by adenine base editors (ABEs). Our results demonstrate that ABE efficiently corrects the pathogenic allele in patient-derived fibroblasts, restoring therapeutic levels of β-gal activity. Off-target DNA analysis did not detect off-target editing activity in treated patient's cells, except a bystander edit without consequences on β-gal activity based on 3D structure bioinformatics predictions. Altogether, our results suggest that gene editing might be an alternative strategy to cure GM1 gangliosidosis.

Introduction

Over the last two decades, high-throughput sequencing (HTS) technology has accelerated the identification of genetic alterations involved in human diseases, thus allowing many patients to benefit from an accurate diagnosis. Despite this historical breakthrough, a high number of diagnosed patients are currently awaiting personalized therapy. The development of curative gene therapies for these patients is indispensable.[1] According to ClinVar, ~54,500 human pathogenic genetic variants have been associated with diseases and more than 58% are single nucleotide variants (SNVs) (https://www.ncbi.nlm.nih.gov/clinvar/). This observation suggests that gene editing strategies aimed at correcting the root cause of disease could be an alternative strategy to cure disease instead of classical gene therapies aimed at bringing a novel functional copy of the altered genes.[2,3]

Nowadays, gene editing approaches such as base and prime editing (BE and PE) enable specific restoration of a functional gene by correcting pathogenic variants.[3] BE has been successfully used to cure multiple diseases in different models and species.[4–8] To date, the most advanced application in humans is to cure sickle cell anemia through *ex vivo* targeting of hematopoietic stem and progenitor cells from patients.[5] BE also shows promise in limiting the deleterious effect of progerin (SNV altering the *Lamin A* mRNA splicing), as recently demonstrated in a murine progeria model,[8] and to lower cholesterol in serum of primates by turning off the *PCSK9* gene.[7,9]

Although this innovative gene editing approach is promising, it is important to keep in mind the editing efficiency, the potential off-target effects, and the challenge in reaching all targeted cells *in vivo*.[10,11] To date, BE has the best

[1]*INSERM U1242, OSS, Univ Rennes, Rennes, France;* [2]*CHU Rennes, Service de Génétique Clinique, Centre de Référence Maladies Rares CLAD-Ouest, FHU GenOMEDS, ERN ITHACA, Hôpital Sud, Rennes, France;* [3]*INSERM, EHESP, IRSET–UMR_S, 1085, Université Rennes 1, Rennes, France;* [4]*Service de Cytogénétique et Biologie Cellulaire, CHU Rennes, Rennes, France;* [5]*Department of Pediatrics, Competence Center of Inherited Metabolic Disorders, Rennes Hospital, Rennes, France;* [6]*Laboratoire de Génétique Moléculaire et Génomique, Centre Hospitalier Universitaire de Rennes, Rennes, France;* [7]*Univ Rennes, CNRS, IGDR (Institut de Génétique et Développement de Rennes), UMR 6290, ERL U1305, Rennes, France;* [8]*Laboratoire de Biochimie, CHU de Toulouse, Pôle biologie, Institut Fédératif de Biologie, Toulouse, France;* [9]*CHU Lyon HCL, LBMMS–Service Biochimie et Biologie Moléculaire, UM Pathologies Héréditaires du Métabolisme et du Globule Rouge, Bron, France;* [10]*Univ Rennes, CNRS, ISCR (Institut des Sciences Chimiques de Rennes)–UMR 6226, Rennes, France;* [11]*Department of Chemistry and Molecular Biology, University of Gothenburg, Göteborg, Sweden; and* [12]*Department of Ophthalmology, CHU Rennes, Univ Rennes, Rennes, France.*

*Address correspondence to: *David Gilot, INSERM U1242, OSS, Univ Rennes, avenue Bataille Flandres-Dunkerque, Rennes 35000, France,* E-mail: david.gilot@univ-rennes1.fr

efficiency rate compared to PE or CRISPR-Cas9 coupled to a donor. However, only C-to-T (CBE) and A-to-G (ABE) BE methods are fully validated for gene therapy.[12,13]

Moreover, CBE and adenine base editor (ABE) deaminases are active on a wide editing window. Indeed, the maximum deaminase activity extends from nucleotide 4 to 6 from the 5′ end of the sgRNA depending on the BE version. This point suggests that proximal C or A nucleotides should be edited into T or G within the editing window, depending on the genomic context.[14,15] Consequently, two kinds of editing events might occur with BEs: the expected on-target edit and the unwanted on-target one(s) called bystander edit(s). Although these bystander events are sometimes unavoidable, plenty of strategies have been proposed and published to improve BE window specificity and reduce their occurrence.[16,17]

To facilitate the design of sgRNAs for BE applications, several improvements have been implemented such as less stringent protospacer adjacent motif (PAM) than the canonical 5′-NGG-3′ (such as NRN and NYN PAM; SpRY Cas enzyme) and high-fidelity (HF) BE Cas enzymes.[18,19] So the latest generation of BEs is characterized by a high efficiency rate of editing and a low level of off-target edits since these Cas9s cleave only one DNA strand (nickase) and are sometimes HF, making them exploitable for gene therapy.[20]

In humans, CBE and ABE should, respectively, correct, *in theory*, 14% and 47% of GLB1 pathogenic variants.[3] In this study, we investigated whether BE may constitute an alternative strategy to cure GM1 gangliosidosis. Indeed, there is currently no effective therapy, and only supportive treatments can be offered.[21] GM1 gangliosidosis is an autosomal recessive lysosomal storage disorder estimated to occur in 1 in 100,000 to 200,000 newborns.[22] There are four different types of GM1 gangliosidosis based on the age when symptoms first appear and the severity of disease progression. Defects in the *GLB1* gene (coding the β-galactosidase [β-gal]) cause impaired enzyme activity leading to the toxic accumulation of gangliosides and neurodegeneration that presents as cognitive impairment, paralysis, and early death.

Three ongoing clinical trials (NCT03952637, NCT04273269, and NCT04713475) aim to deliver a functional copy of the *GLB1* gene to slow down or stop disease progression (classical gene therapy), but cannot reverse the damage already caused by the disease. For two clinical trials, the *GLB1* cDNA is carried by adeno-associated viral (AAV) vector injected into the cisterna magna to reach the neuronal cells through the cerebrospinal fluid and to break down GM1 ganglioside. Preclinical studies clearly demonstrated the ability of AAV to transport genes into neuronal cells, suggesting that these vectors should also bring both BE and sgRNA.[23–25]

Transgenes transferred by this type of vectors are transcriptionally active and are maintained as an extra-chromosomal (episomal) form in the transduced cells for a long-term period.[24] However, the preclinical trials have been mainly performed in short lifespan animals such as mice and felines, making it difficult to evaluate the long-term beneficial effect required for patients.[24,26–29] These studies mainly demonstrated a reduction of lysosomal storage in the central nervous system and an extended lifespan for these animal models.

To the best of our knowledge, the long-term expression of *GLB1* in large animal models through AAV vectors has not been investigated. In other words, it is unknown how long the therapeutic effect will last following the initial establishment of transgene expression, although animal and emerging human data show that the expression can be maintained for at least 10 years in muscles.[30] The durability of therapeutic response is key to long-term treatment success, especially since immune responses to AAV vectors may prevent re-dosing with the same therapy.[31]

In this study, we show that 82% of genetic alterations of *GLB1* gene are SNVs. Among the pathogenic variants, 41% could be targeted by ABE. As a proof-of-concept experiment, we designed and validated *in vitro* an ABE strategy for a young patient with GM1 gangliosidosis. Based on the ABE efficiency and the quantification of off-target edits, our data suggest that gene editing is an alternative strategy to cure GM1 gangliosidosis.

Methods

Editorial policies and ethical considerations

Written informed consent was obtained from the patient and his parents. All procedures were in accordance with the ethical standards of the Ethics Committee of Rennes University Hospital and the French law (CCTIRS Comité Consultatif sur le Traitement de l'Information en matière de Recherche dans le domaine de la Santé). Peripheral blood samples (for DNA extraction) and skin biopsies (for functional analyses and personalized gene therapy development) were collected from all the participants.

Exome sequencing and bioinformatics pipeline

Trio exome sequencing was performed at Rennes Hospital University (Molecular Genetics and Genomics Laboratory) using standard pipeline as previously described.[32] Identified pathogenic variants were described according to the Human Genome Variation Society nomenclature guidelines (https://varnomen.hgvs.org/).

Patient-derived fibroblasts: primary culture and immortalization

The fresh skin punch biopsies were dilacerated with scalpels under a sterile area and then transferred into T25 flasks containing 5 mL of AmnioMAX C-100 (Gibco) medium. After 1–2 weeks, explant growing cells were washed with Dulbecco's phosphate-buffered saline (DPBS; Lonza), trypsinized with TrypLE™ Express Enzyme (1×; Gibco), and passaged in T75 flasks for fibroblast amplification. Primary cells were then immortalized by SV40 T antigen lentiviral transduction. Lentiviral particle production was performed in HEK293T cell line by following Trono Lab recommendations (http://tronolab.epfl.ch).

Briefly, psPAX2 (Addgene plasmid ID #12260), pVSVG (Addgene plasmid ID #8454), and pLOX-TtagiresTK plasmids (Addgene plasmid ID #12246) were transfected into HEK293T cells with lipofectamine 2000 (Thermo Fisher Scientific) according to the manufacturer's instructions. Cell supernatant containing lentiviral particles was collected after 2 days, centrifuged, and filtered (0.45 μm) to eliminate HEK293T-derived cell debris. Fibroblasts in primary culture (P6 well plate; Falcon®) were infected with 500 μL of this infectious media in the presence of 8 μg/mL polybrene (Sigma) to achieve viral infection.

Cell culture

Immortalized patient-derived fibroblasts and HEK293T (ATCC) cells were cultured, respectively, in RPMI-1640 medium (Lonza) or Dulbecco's modified Eagle's medium (Gibco), each supplemented with 10% fetal bovine serum (Gibco), 1% glutamine (Lonza), and 1% penicillin-streptomycin (Sigma). When confluent, cells were washed with DPBS (Lonza), digested with TrypLE Express enzyme (1×; Gibco), and subsequently passaged at 1:10 ratio. All cells were maintained at 37°C in a humidified incubator with 5% CO_2. Cell lines were routinely tested for mycoplasma infection with PlasmoTest Mycoplasma Detection Kit (Invivogen) and negative results were obtained.

DNA extraction, polymerase chain reaction, and Sanger sequencing

DNA was extracted from frozen cell pellets with the Nucleospin tissue DNA extraction kit (Macherey-Nagel). DNA concentration was evaluated using the NanoDrop1000 spectrophotometer (Thermo Fisher Scientific). Polymerase chain reaction (PCR) was performed from 50 ng DNA with the Phusion™ High-Fidelity DNA Polymerase kit (Thermo Fisher Scientific). The list of primers is presented in Supplementary Table S1. Samples were subjected to thermal cycling as follows: 98°C for 30 s (initial denaturation step), 98°C for 10 s, primers' annealing temperature for 15 s, 72°C for 30 s (35 cycles), and 72°C for 5 min (final elongation step).

Amplicon size and purity were checked on 1.5% agarose gel electrophoresis before Sanger's reaction. Sanger sequencing was performed directly on 1 μL of PCR reaction in the presence of 0.5 μM primer and the Big Dye Terminator V3.1 (Applied Biosystems™). The following thermocycler program was used: 96°C for 5 min (initial denaturation step), then 96°C for 1 min, primers' annealing temperature for 1 min, and 62°C for 2 min (30 cycles). Sequence products were purified on Sephadex G50 beads (GE Healthcare) and directly loaded onto 3130xl Genetic Analyzer capillary electrophoresis laser coupled system (ABI PRISM).

RNA extraction, reverse transcription, and quantitative PCR

RNA extraction was performed from frozen tissue in culture plates (P6 well plate; Falcon) by using the NucleoSpin RNA kit (Macherey-Nagel). RNA concentration was measured with NanoDrop1000 spectrophotometer (Thermo Fisher Scientific). Reverse transcription was performed on 500 ng total RNA with the High-Capacity cDNA Reverse Transcription kit (Applied Biosystems). Quantitative PCR (qPCR) was performed in 384-well plates on 2.5 ng of reverse-transcribed cDNA using the SYBR Green PCR Master Mix (Applied Biosystems) in the presence of 1 μM of forward and 1 μM of reverse primers, using the QuantStudio 5 quantitative PCR equipment (Applied Biosystems). The primer sequences used are available in Supplementary Table S1. Raw data were extracted with QuantStudio Design and Analysis Software (Applied Biosystems). Relative gene expression compared to control conditions was calculated by using the $2^{-\Delta\Delta}$ Ct method. *GAPDH* was used as a housekeeping gene for normalization.

Protein extraction

Cells were lysed and proteins were extracted from fresh fibroblast cells with RIPA buffer (Thermo Fisher Scientific) supplemented with protease and phosphatase inhibitor mini-tablet (Pierce, Thermo Fisher Scientific). Protein quantification was performed with Pierce BCA protein assay kit (Thermo Fisher Scientific) and absorbance was measured with spark microplate reader (TECAN) at 562 nm.

β-Gal enzymatic activity measurement

β-Gal activity was evaluated using a fluorogenic method initially described by Ho and O'Brien.[33] Briefly, 20 μL of

fresh cell lysates were incubated in a white 96-well microplate (Grenier Bio-One) with 100 μL of buffer solution (pH 4.3) containing 0.5 mM of 4-methylumbelliferyl-β-D-galactopyranoside substrate (Sigma). A kinetic analysis was performed at 37°C for 1–2 h. Every 4 min, the fluorogenic substrate was excited at 366 nm and fluorescence emission, proportional to enzyme activity, was measured at 442 nm with a spark microplate reader (TECAN). Enzyme activity was assessed from the slope of the fluorescence = f (time) curve and normalized per microgram of protein.

Western blot

Protein samples were reduced and denatured with lithium dodecyl sulfate and reducing agent for 10 min at 70°C. Then, 20 μg of each sample was loaded in 4–12% Bis-Tris Gel (NuPAGE; Invitrogen) and migration was done with following parameters: 1 h 30 min, 200 V, and 400 mA. Proteins were then transferred onto a nitrocellulose membrane (Invitrogen™ iBlot™ Transfer Stack) with iBlot transfer device system (Invitrogen).

After transfer and incubation with a blocking solution (1 h at room temperature, TBS-Tween 0.1%; 5% bovine serum albumin; Eurobio), the membrane was probed with the primary antibody overnight at 4°C (rabbit anti-β-galactosidase antibody, 15518-1-AP Protein Tech, dilution 1/1000; and mouse anti-α-tubulin, dilution 1/10,000; T6199 Sigma-Aldrich) and then for 1 h at room temperature with the horseradish peroxidase (HRP)-linked secondary antibody (HRP-linked anti-rabbit IgG, dilution 1/2000; #7074 Santa Cruz; and HRP-linked anti-mouse IgG, dilution 1/2000; #7076 Santa Cruz). Signal was detected with Amersham ECL select substrate (Cytiva) under a luminescent image analyzer (ImageQuant LAS 4000). Uncropped western blots are available in Supplementary Figure S1.

Cloning

Single guide RNAs were designed according to the recommendations of Walton et al,[19] Supplementary Table S1. Designed oligonucleotides were integrated into BPK1520 backbone (Addgene plasmid ID #65777) by golden gate assembly as previously described.[34] Plasmids were transformed into NEB® Stable competent *Escherichia coli* C3040H (New England BioLabs) by following the manufacturer's recommendations. Bacteria were seeded onto ampicillin (100 μg/mL) Lysogeny broth (LB) agar plates and incubated overnight at 37°C. Isolated colonies were then amplified overnight at 37°C with LB growth medium and ampicillin (100 μg/mL) under constant agitation. Plasmid DNA was purified with NucleoBond® Xtra Maxi kit (Macherey Nagel) according to the manufacturer's instructions. Constructs were verified by Sanger sequencing. The plasmid encoding the sgRNA number 8 used in this study is available on Addgene (BPK1520-sgRNA GLB1; Addgene #184378).

ABE transfection

Immortalized fibroblasts were seeded in 6-well plates (Falcon) (500,000 cells/well). Approximately 24 h after seeding (~60% confluency), cells were transfected with 11.55 μL of Viafect reagent (Promega) according to the manufacturer's protocols with 2200 ng of ABEmax(7.10)-SpRY-P2A-EGFP plasmid (Addgene plasmid ID #140003) and 1100 ng of sgRNA plasmid (Addgene plasmid ID #65777). The medium was replaced 6 and 24 h after transfection to eliminate dead cells. Forty-eight hours after transfection, cells were washed with DPBS (Lonza), digested with TrypLE Express enzyme (Gibco), and resuspended into RPMI-1640 medium (Lonza). GFP positive cells were sorted by fluorescence-activated cell sorting (FACS, FACSAria FUSION; Becton Dickinson). Sorted cells were either lysed for DNA extraction and HTS or individualized by limit dilution for clonal amplification (96-well plates, 1 cell/well; Falcon).

Approximately 3 weeks after the limit dilution, pure clones were amplified in 12-well plates (Falcon). To easily identify the edited cells, β-galactosidase assays were performed and gene editing was confirmed by Sanger sequencing.

siRNA transfection

Immortalized fibroblasts were seeded in 6-well plates (500,000 cells/well; Falcon). Approximately 24 h after seeding (~60% confluency), cells were transfected with 50 nm siRNA CTRL or siRNA *GLB1* (IDT, sequence available in Supplementary Table S1) with lipofectamine RNAimax (Thermo Fisher Scientific) according to the manufacturer's instructions. Forty-eight hours after transfection, cells were stored at −80°C and proteins were then extracted.

Off-target identification (CRISPOR)

Off-target sites were predicted bioinformatically by using the CRISPOR online tool (http://crispor.tefor.net).[35] Putative off-target sites were ranked according to cutting frequency determination (CFD) score[36] and top 10 off-target hits were selected for deep sequencing (amplicons) (data are available in Supplementary Table S3). In addition, putative exonic off-target sites were checked by exome sequencing.

Amplicon HTS

Genomic regions of interest were amplified by PCR (Phusion High-Fidelity DNA Polymerase; Thermo Fisher Scientific or KAPA2G Robust HotStart PCR; Sigma) from genomic DNA samples. Amplicons were purified with AMPure XP magnetic beads (Beckman Coulter). The library was prepared with the SureSelect XT HS2 DNA kit (Agilent). We followed the manufacturer's recommendations (except that initial DNA fragmentation, hybridization, and capture steps were skipped). Pooled libraries were sequenced on a MiSeq instrument (Illumina) with a 2×250 bp paired-end running method (MiSeq Reagent Nano Kit v2 500 cycles; Illumina). The flow cell was loaded with 5 pM pooled libraries containing 5% PhiX control V3 (Illumina). Raw sequencing data were demultiplexed with Bcl2Fastq software (v2.19; Illumina) (data are available in Supplementary Table S3).

CRISPResso2

FastQ files were submitted to CRISPResso2[37] for precise editing quantification. We used the following parameters: -wc = −10, -q = 30, - -min-bp-quality-or-N = 30, - -conversion-nuc-from = A, and - -conversion-nuc-to = G. The matrix ''selected-nucleotide-percentage-table-around-sgRNA'' generated by CRISPRESSO was used to calculate the potential editing percentage. For both on-target and off-target data, the line with nucleotide ''N'' (Q score <30) was removed with a Python script (Supplementary Fig. S2) to avoid potential editing underestimation (data are available in Supplementary Table S4).

Three-dimensional structure prediction

Maestro Software (Schrödinger Release 2021-3; Schrödinger, LLC, New York, NY, 2019) was used for visualization, basic molecular modeling steps (protein preparation, energy minimization, etc.), as well as for the molecular dynamic (MD) simulation trajectory using Desmond.[38] Crystal structure of the GLB1 protein in complex with galactose (PDB ID: 3THC) served as the starting point for molecular modeling. The protein preparation wizard was used to prepare the crystal structure as follows: hydrogen atoms were added and possible metal binding states generated.

The protonation and tautomeric states of Asp, Glu, Arg, Lys, and His were adjusted to match a pH of 4.3 and possible orientations of Asn and Gln residues were generated. Hydrogen bond sampling with adjustment of active site water molecule orientation was performed using PROPKA. Water molecules with fewer than three hydrogen bonds to nonwater molecules were deleted. Finally, the protein-ligand complexes were subjected to geometry refinements using the OPLS4 force field[39] in restrained minimizations. The S302G mutant was then generated using the ''Residue and Loop mutation'' tool included with maestro, followed by an energy minimization of the whole structure in implicit water.

The GLB1 wild-type (WT) and S302G structures were then prepared for MD with the system builder panel using the following parameters: each system was solvated with TIP3P water[40] under periodic boundary conditions with the minimum distance between any atom in the solute and the edge of the periodic box being 10.0 Å; Na^+/Cl^- counterions were added as appropriate for the neutralization of the system; 0.154 M NaCl. MD simulations for each system were performed with Desmond as follows: 3×100 ns total time; OPLS4 force field; 100 ps trajectory recording intervals; system energy set to 1.2, NPT ensemble class; 300.0K; 1.01325 bar; and model relaxed before simulation. Quality control of our simulations was done using the ''Simulation Quality Analysis'' tool as well as the ''Simulation Interactions Diagram'' tool.

Statistical analysis

All data are expressed as the mean − standard error of the mean of at least three individual experiments, excepting the HTS experiments. Data were analyzed by Student's t-test using GraphPad Prism v8.0.1 (GraphPad Software, San Diego, CA). p-Values were deemed to be statistically significant as follows: $*p<0.05$; $**p<0.01$;$***p<0.001$; $****p<0.0001$. All raw data are available in Supplementary Table S5.

Results

We investigated here whether genome edition could be a credible approach to treat GM1 gangliosidosis by correcting *GLB1* SNVs.

GLB1 genetic variants

First, we analyzed the genetic alterations of the *GLB1* gene found in ClinVar to characterize the origin of GM1 gangliosidosis (Fig. 1 and Supplementary Table S2). The *GLB1* variants are almost exclusively germline (>95%) SNVs (82%), the majority of which are missense (60%) and some frameshift (11%) (Fig. 1A–C). It is interesting to note that the *GLB1* noncoding sequence is also impacted (untranslated region and splice sites; ∼20%).

Next, we focused on the 93 known pathogenic variants (class 5 corresponding to 17% of all variants, $N=532$) to estimate the ability of BE and PE to correct them (Fig. 1D, E). Importantly, PE, ABE, and CBE should, in theory, correct up to 100, 41, and 15%, respectively,

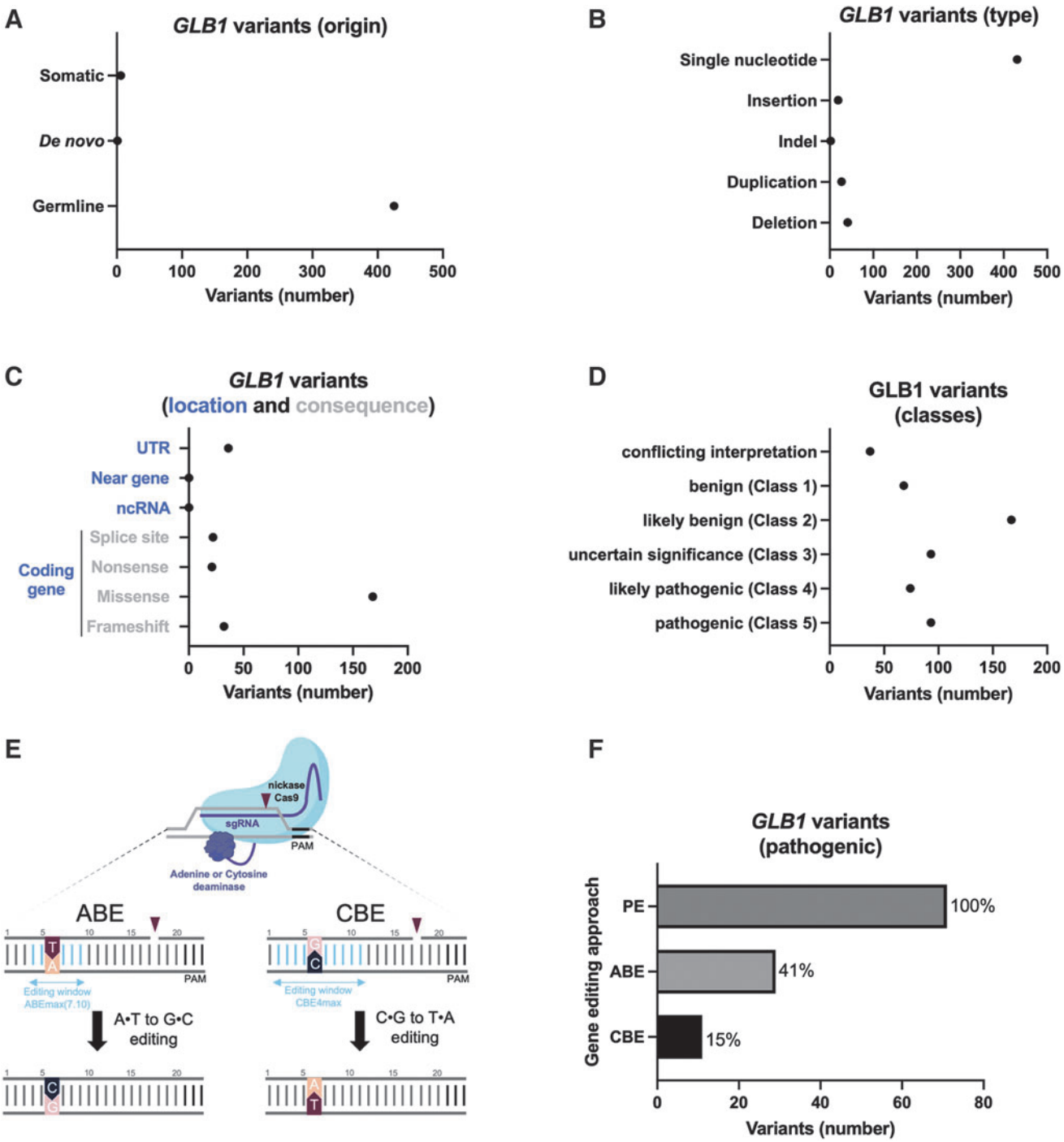

FIG. 1. Genetic alterations of *GLB1*. **(A)** Origin of the *GLB1* variants (somatic, *de novo*, or germline), **(B)** types of *GLB1* variants, **(C)** location and consequence of *GLB1* variants, **(D)** number of *GLB1* variants in the different classes, **(E)** scheme recapitulating base editor effects (ABE and CBE), **(F)** number of *GLB1* variants (class 5) that might be edited by PE, ABE, or CBE. ABE, adenine base editor; CBE, cytosine base editor; PE, prime editing.

of *GBL1* pathogenic variants described in ClinVar (Fig. 1F). Of course, the genomic context of each variant must be taken on a case-by-case basis to consider compatibility with editing window and PAM of specific editors. Since BE is currently the most efficient approach for gene editing in humans,[3] we evaluated the ability of ABE to correct a missense variant associated with GM1 gangliosidosis as a proof-of-concept experiment. We selected a patient with a missense variant targetable by ABE (Fig. 2).

GLB1 characteristics of the patient

The patient is the second child of nonconsanguineous parents (Fig. 2A). He has one healthy brother. Pregnancy and delivery were uneventful. He was born at 40 weeks of gestation, and his birth weight was 4015 g. He achieved motor skills with slight delay, as he was able to sit at 9 months, to stand up at 19 months, and to make his first steps at 22 months of age (Fig. 2A). At 30 months of age, he began to lose previously acquired milestones as he could no longer walk independently. Regarding speech development, he could pronounce his first words at the end of his first year of age, but he did not progress further and progressively lost speech during the following months.

At 22 months of age, the parents noticed some episodes of eyelid shaking. The ophthalmologic examination was normal. A first brain magnetic resonance imaging (MRI) was performed at 23 months of age showing normal results. At 3 years of age, generalized epilepsy became obvious. Initial anticonvulsant therapy by Levetiracetam was switched to valproic acid due to side effects. Follow-up cerebral MRI at 3 years of age showed generalized brain atrophy and hypomyelination.

The first genetic investigations, which included screening for Steinert disease, Angelman and Prader Willi syndrome, and CGH array analysis, were normal (data not shown). Trio whole exome sequencing (WES) of the child and his parents identified two heterozygous probable pathogenic variants in the *GLB1* gene (NM_000404.2): c.907G>A (p.Val303Met) and c.75+2 dup, inherited from his mother and father, respectively (Fig. 2B, C). The first variant is a missense variant (never described) and the second is located at a splice site, leading to a 20-nucleotide intron retention in *GLB1* RNA.[41]

Since the *GLB1* genetic alterations suggested an altered β-gal activity associated with GM1 gangliosidosis, we evaluated it in white blood cells. Analyses revealed a pathogenic drop of β-gal activity (8 nmol/h/mg of proteins in the patient vs. control: 197 nmol/h/mg of proteins, data not shown). The residual β-gal activity was estimated to be 4% of control. As a control, the neuraminidase activity was similar for the patient and the control sample (data not shown). Thus, the abnormal β-gal activity supported the pathogenicity of the two variants identified in *GLB1* and led to the diagnosis of a late-onset form of infantile GM1 gangliosidosis for this patient.

To confirm this diagnosis, three skin biopsies were performed to generate primary fibroblast cultures (parents and patient) (Fig. 2D). To obtain enough cells, we immortalized these fibroblasts using T antigen from SV40 by a lentiviral transduction.

In accordance with results obtained with Peripheral Blood Mononuclear Cells, we confirmed that patient's fibroblasts displayed an undetectable β-gal activity in our experimental conditions (Fig. 2E). In contrast, the β-gal activity detected in fibroblasts isolated from the parents was reduced by 50% when compared to control

FIG. 2. Characterization of patient-derived fibroblasts. **(A)** Milestones of the patient with GM1 gangliosidosis, **(B)** GM1 gangliosidosis patient pedigree, indicating autosomal recessive inheritance (genealogical tree), **(C)** hypothetical effect of inherited variants on *GLB1* mRNA and amino-acid sequence, **(D)** workflow describing patient-derived fibroblast purification and immortalization using SV40 T antigen (transduced by lentivirus), **(E)** β-galactosidase activity in patient-derived fibroblasts. The measured values of the patient were compared to the values obtained from his parents and a control case (control fibroblasts), $n \geq 3$ biologically independent experiments, each histogram represents the mean ± SD. **(F)** GLB1 protein levels in the same fibroblasts. Specificity of the GLB1 antibody raised against GLB1 protein was evaluated using siRNA targeting *GLB1* mRNA or a nontargeting siRNA (siCTR). Western blot results are representative of at least three experiments and α-tubulin serves as a loading control, **(G)** expression levels of *GLB1* mRNA evaluated by RT-qPCR in patient-derived fibroblasts or control fibroblasts, **(H)** allele-specific qPCR quantification in patient-derived fibroblasts (ΔCt). Otherwise indicated, data were subjected to Student's *t*-test and *p*-values were deemed to be statistically significant as follows: $^{*}p < 0.05$; $^{**}p < 0.01$;$^{***}p < 0.001$; $^{****}p < 0.0001$. Raw data are available in Supplementary Table S5. NMD, nonsense-mediated mRNA decay; RT-qPCR, real-time quantitative reverse transcription PCR; SD, standard deviation.

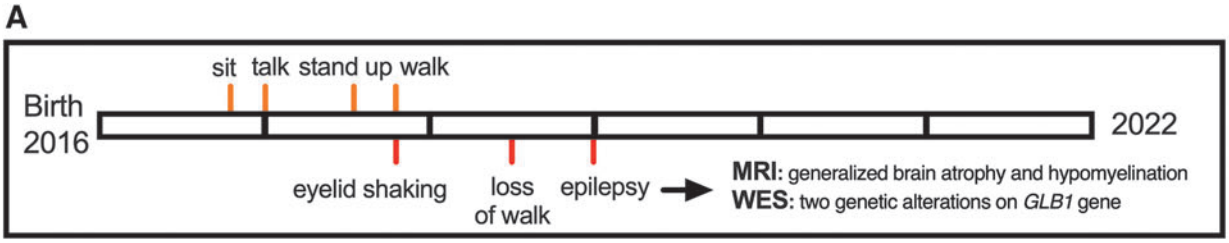
A
sit talk stand up walk
Birth
2016
2022
eyelid shaking
loss of walk
epilepsy
MRI: generalized brain atrophy and hypomyelination
WES: two genetic alterations on GLB1 gene

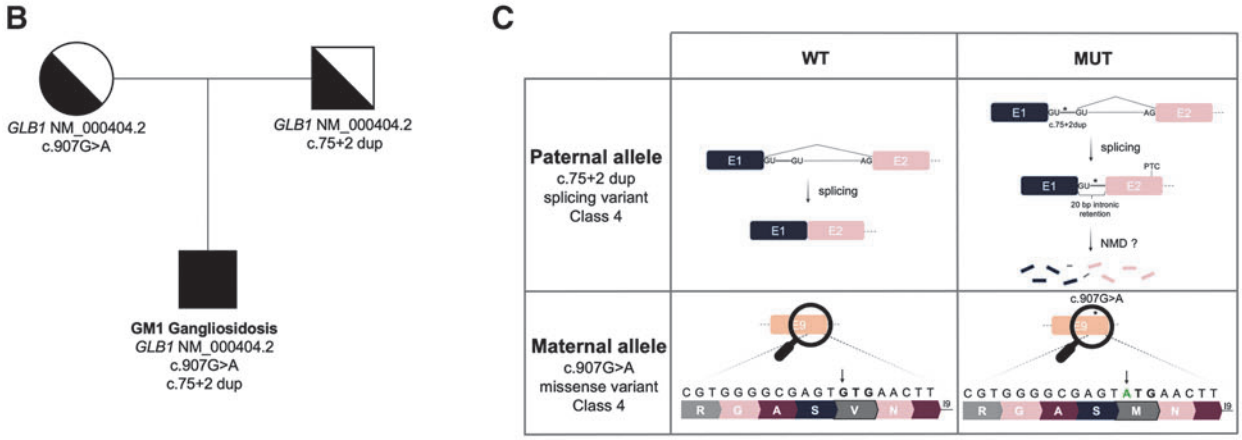
B
GLB1 NM_000404.2
c.907G>A
GLB1 NM_000404.2
c.75+2 dup
GM1 Gangliosidosis
GLB1 NM_000404.2
c.907G>A
c.75+2 dup
C
WT
MUT
Paternal allele
c.75+2 dup
splicing variant
Class 4
splicing
NMD ?
Maternal allele
c.907G>A
missense variant
Class 4
c.907G>A

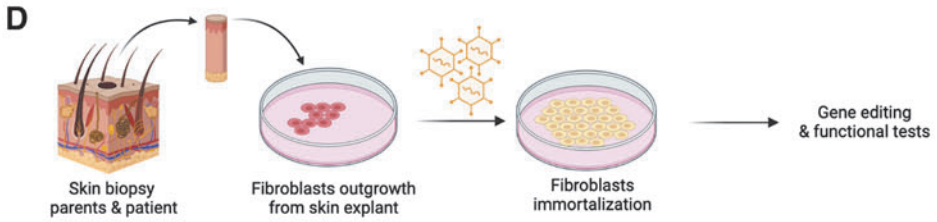
D
Skin biopsy
parents & patient
Fibroblasts outgrowth
from skin explant
Fibroblasts
immortalization
Gene editing
& functional tests

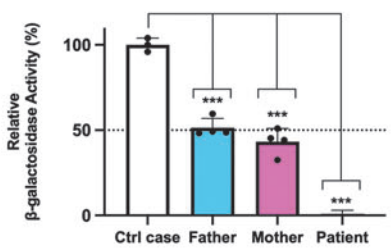
E
Relative
β-galactosidase Activity (%)
100
50
0
***
Ctrl case
Father
Mother
Patient

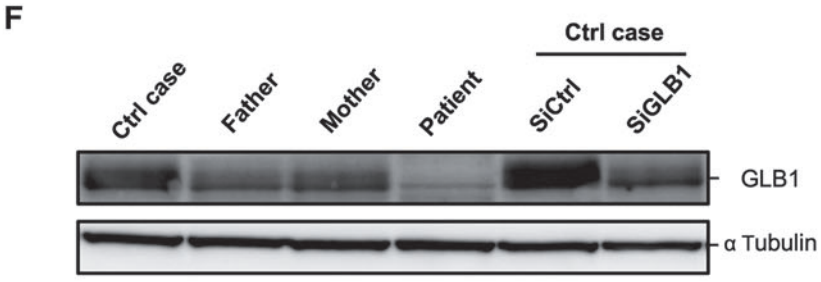
F
Ctrl case
Ctrl case
Father
Mother
Patient
SiCtrl
SiGLB1
GLB1
α Tubulin

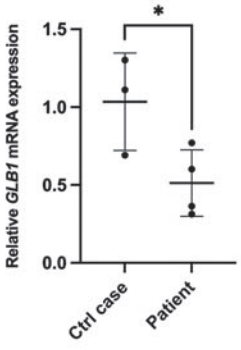
G
Relative GLB1 mRNA expression
1.5
1.0
0.5
0.0
*
Ctrl case
Patient

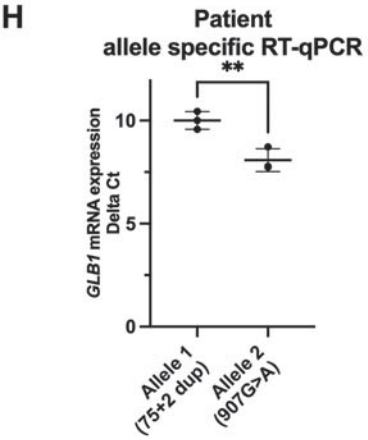
H
Patient
allele specific RT-qPCR
GLB1 mRNA expression
Delta Ct
10
5
0
**
Allele 1
(75+2 dup)
Allele 2
(907G>A)

fibroblasts. These results demonstrated that the combination of these two inherited mutations abrogated the β-gal activity and expression (Fig. 2F). Next, we confirmed a reduced amount of *GLB1* mRNA in patient-derived fibroblasts when compared to control fibroblasts (Fig. 2G) and both alleles were detectable (Fig. 2H). Allele 1 (c:75 + 2dup) has reduced expression compared to allele 2, probably due to nonsense-mediated decay of transcript containing 20 bp of intronic sequence as already suggested.[41] In conclusion, we showed that the combination of these two genetic alterations explains this case of GM1gangliosidosis.

Adenine base editing strategy for GM1 gangliosidosis

To conceive a therapeutic solution for this patient, we selected the ABE approach to correct only one allele; the *GLB1* c.907G>A (p.Val303Met) mutation (maternally inherited), aiming to restore a β-gal activity (50%) as found in his asymptomatic parents (Fig. 3A). The ABE strategy is known to reach a greater efficiency than PE, and ABE is already used in clinical trials.[3] Only a PE approach has the potential to repair the other genetic alteration inherited from the father.[42]

To optimize our chance of designing effective sgRNA for ABE, we selected the human codon-optimized ABEmax(7.10): A-to-G base editor with nSpCas9 SpRY (D10A/L1111R/D1135V/G1218R/E1219F/A1322R/R1335V/T1337R).[19] The main advantage of this Cas9 variant is that the classical NGG PAM evolves to NRN or NYN, with NRN PAM being better recognized than NYN PAM (NRN>NYN). Using this near-PAMless engineered CRISPR-Cas9 variant, we successfully designed and cloned two sgRNAs (Fig. 3A–C). Next, ABEmax(7.10) and one sgRNA were transfected into immortalized fibroblasts derived from the patient (Fig. 3D).

Transfected cells were selected using the enhanced green fluorescent protein (EGFP) signal encoded by the plasmid pCMV-T7-ABEmax(7.10)-SpCas9-NG-P2A-EGFP (Fig. 3D). Five days after the enrichment of transfected cells ($EGFP^+$-sorted cells), the BE efficiency was estimated by DNA sequencing as previously described.[6,37] CRISPResso2 analyses indicated that A907 was converted into G907 (reference nucleotide) in ∼52% of reads from the maternal allele as expected with this BE approach (Fig. 3E). The sgRNA 7 was inefficient (Supplementary Table S4), confirming the requirement to evaluate several sgRNAs for BE.

Next, we performed a clonal selection to isolate edited G907 clones (on-target edit). β-Gal activity and β-gal protein levels were assessed (Fig. 3F). For the six clones exposed to the sgRNA8, ABE rescued a therapeutic level of β-gal protein and β-gal activity when compared to donor cells (wt *GLB1*). The restored β-gal activity reached a similar activity to that detected in the fibroblasts isolated from his asymptomatic parents (50% of the normal values) (Fig. 2E).

Window editing of ABE

Closer inspection of our sequencing results indicated that A904 (position A_5 from the 5′ sgRNA extremity) is also converted into G904 (∼31% of the reads) (Figs. 3F and 4A, B). This result could be explained by the active window of the ABEmax (7.10), which extends from nucleotides N_4 to N_9 (Fig. 3B).[19] In parallel, we did not detect any significant editing event outside this editing window by NGS (raw data Supplementary Table S4).

Since the clone#20 (G907-G904; on-target and bystander edits) displayed a similar β-gal activity than

FIG. 3. Adenine base editing strategy for GM1 gangliosidosis. **(A)** Maternal inherited *GLB1* variant is targetable by ABE, **(B)** scheme explaining the base editor window. Potential bystander edit might be obtained (proximal adenine to the on-target adenine located in the base editor window), **(C)** two sgRNA were designed to correct the pathogenic **A**TG (Met) into the **G**TG (Val) on exon 8 of *GLB1* gene using ABE, **(D)** workflow used to evaluate the ABE efficiency and specificity for the patient-derived fibroblasts, **(E)** efficiency of ABE to introduce the on-target edit ($A_8 \rightarrow G_8$ or 907A→G) using the sgRNA8 in fibroblasts. Results were obtained by amplicon deep sequencing and analyzed by CRISPResso2. Bystander edits were identified. **(F)** Clones isolated after transfection sgRNA8+ABE or sgRNA CTR+ABE were compared to normal fibroblasts or untreated patient-derived fibroblasts. Each clone was characterized for β-galactosidase activity, β-galactosidase protein, and edits. $n = 3$ biologically independent experiments, each histogram represents the mean ± SD. α-Tubulin serves as a loading control. Data were subjected to Student's *t*-test and *p*-values were deemed to be statistically significant as follows: $^*p < 0.05$; $^{**}p < 0.01$;$^{***}p < 0.001$; $^{****}p < 0.0001$. Raw data are available in Supplementary Table S5. MUT, mutated; WT, wild type.

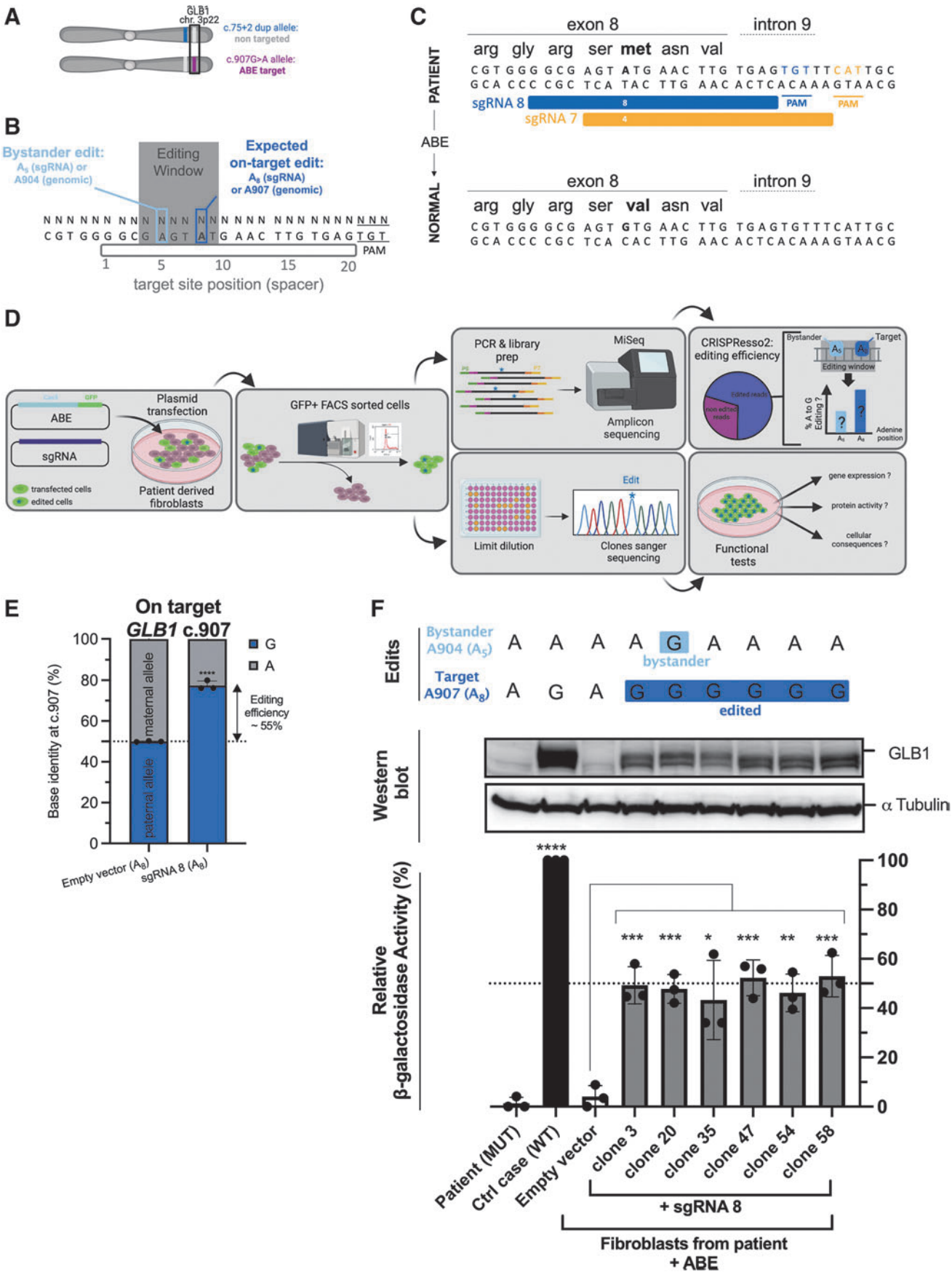
A
GLB1
chr. 3p22
c.75+2 dup allele:
non targeted
c.907G>A allele:
ABE target
B
Bystander edit:
A5 (sgRNA) or
A904 (genomic)
Editing Window
Expected
on-target edit:
A8 (sgRNA)
or A907 (genomic)
NNNNNN NNN NNN NNN NNNN NNN NNNNNNNNN
CGT GGG GCG AGT ATG AAC TTG TGAGTGT
PAM
1 5 10 15 20
target site position (spacer)
C
PATIENT
ABE
NORMAL
exon 8
intron 9
arg gly arg ser met asn val
CGT GGG GCG AGT ATG AAC TTG TGAGTGTTTCATTGC
GCA CCC CGC TCA TAC TTG AAC ACTCACAAAGTAACG
sgRNA 8
sgRNA 7
PAM
PAM
exon 8
intron 9
arg gly arg ser val asn val
CGT GGG GCG AGT GTG AAC TTG TGAGTGTTTCATTGC
GCA CCC CGC TCA CAC TTG AAC ACTCACAAAGTAACG
D
ABE
sgRNA
transfected cells
edited cells
Plasmid transfection
Patient derived fibroblasts
GFP+ FACS sorted cells
PCR & library prep
MiSeq
Amplicon sequencing
CRISPResso2: editing efficiency
Bystander
Target
Editing window
Edited reads
non edited reads
% A to G Editing
Adenine position
Limit dilution
Edit
Clones sanger sequencing
Functional tests
gene expression ?
protein activity ?
cellular consequences ?
E
On target
GLB1 c.907
Base identity at c.907 (%)
maternal allele
paternal allele
G
A
Editing efficiency ~ 55%
Empty vector (A8)
sgRNA 8 (A8)
F
Edits
Bystander A904 (A5)
A A A A G A A A A
bystander
Target A907 (A8)
A G A G G G G G G
edited
Western blot
GLB1
α Tubulin
Relative β-galactosidase Activity (%)
Patient (MUT)
Ctrl case (WT)
Empty vector
clone 3
clone 20
clone 35
clone 47
clone 54
clone 58
+ sgRNA 8
Fibroblasts from patient
+ ABE

other edited clones (G907-A904; only on-target edit), we investigated the neutral role of this unwanted edit.

We predicted the 3D structure of GLB1 protein (Supplementary Fig. S3). *In silico* mutation followed by an energy minimization of the whole structure showed minimal impact on the surrounding residues and GLB1 structure ($RMSD_{all\text{-}atoms} = 0.720$ Å). To study the potential impact of this mutation more in depth, MD simulations were carried out (3×100 ns) on GLB1 WT and S302G (Supplementary Fig. S3A). Analysis of trajectories did not reveal any significant change in the secondary of tertiary structure of GLB1 (Supplementary Fig. S3B). Altogether, our results strongly suggest that this unwanted on-target event (bystander edit) might have no impact on GM1 gangliosidosis patients.

ABE: off-target detection

Base editors are known to generate bystander edits on surrounding A or C (window editing) (Figs. 3 and 4A). They can have negligible consequence as demonstrated in this study or be avoided by targeting a region without modifiable surrounding bases. However, the off-target edits due to an imperfect sgRNA base pairing to DNA might impair the clinical development of an sgRNA coupled to a base editor.

To uncover genomic loci with the potential for off-target editing, a computational prediction was used (CRISPOR) (Fig. 4A).[35] In total, 978 candidate sites were predicted, including only 63 exonic sites (Supplementary Table S3). Since it remains difficult to evaluate all these potential sites, we ranked them according to the CFD score as previously published.[6] We focused on the top 10 CFD scores (only one is located in an exon; *IDH1* gene, Supplementary Table S3) and off-target effects were investigated by deep sequencing (amplicon-seq). Amplicons were analyzed by CRISPResso2 as previously done for BE efficiency measurement (Fig. 3E).

These samples were stringently quality filtered with a flag for minimum average read quality of 30 (phred33 score = 30) to ensure SNP calling was only performed on high-quality reads. In our conditions, no off-target edit was found for the sgRNA8 in patient-derived fibroblasts. We failed to amplify the OT2 region by PCR. Thus, 9 among the top 10 CFD score sites were investigated (Fig. 4C). To reinforce this result, we performed WES (clone #58 and #20 vs. sgRNA control-transfected cells). On the 63 exonic predicted off-target sites, 32 sites were covered by WES. Under our conditions, no off-target edit was found for the sgRNA8 in patient-derived fibroblasts (0/32). In total, 41 potential off-target sites, including those with the highest CFD scores, were analyzed. We did not find any off-target effect using this protocol.

In addition, we quantified indel events around sgRNA from HTS (amplicons) data followed by CRISPResso2 analysis (Supplementary Fig. S4). On average, indel events remain very low ($\simeq 0.1\%$) compared to on-target editing, which is in accordance with previous reports (Supplementary Fig. S4A, B).[15] Indel size varies approximately from 1 to 20 bases (Supplementary Fig. S4C). Altogether, our results (*in vitro*) strongly suggest that BE might be useful to cure GM1 gangliosidosis.

Discussion

Currently, no curative treatment for GM1 gangliosidosis is available. In theory, therapies should slow or stop the progression of this disease.[21,24] We suspect that the earlier the patient is managed, the greater the therapeutic success will be. The three ongoing clinical trials aim at bringing a healthy *GLB1* coding sequence into the cells of the brain and spinal cord (AAV vector injections into the cisterna magna). To date, it is not possible to evaluate the number of nervous system cells that will be targeted by this classical gene therapy approach (efficiency). Patient follow-up is necessary to determine disease progression and potential adverse effects.

In this study, we provide an *in vitro* proof-of-concept study, strongly suggesting that genome editing can be an alternative strategy for this deleterious disease. To vehiculate the sgRNA and the ABE, the same AAV vector used for ongoing clinical trials[24,25] might be used for a single exposure. To obtain an optimal effect, the injection (genome editing) should be applied as soon as possible after birth, as already done for another neuronal disease using antisense oligonucleotides.[43]

However, viral delivery of base editors allows sustained expression in transduced cells, which may increase the frequency of off-target editing.[44,45] In addition, using

FIG. 4. Specificity assessment of ABE for *GLB1* therapy. **(A)** Scheme recapitulating our workflow to identify the on-target and bystander edits on the *GLB1* gene (base editor window), **(B)** workflow explaining the off-target effects of ABE in patient-derived fibroblasts. Potential off-target edits were predicted by CRISPOR and 41 potential sites were examined by combining whole exome sequencing and amplicon sequencing results. CFD score.[35,36] **(C)** Analysis of the top 10 off-target predicted sites for sgRNA8+ABE. Data were subjected to Student's *t*-test and *p*-values were deemed to be statistically significant as follows: ****$p < 0.0001$. Raw data are available in Supplementary Table S5. CFD, cutting frequency determination.

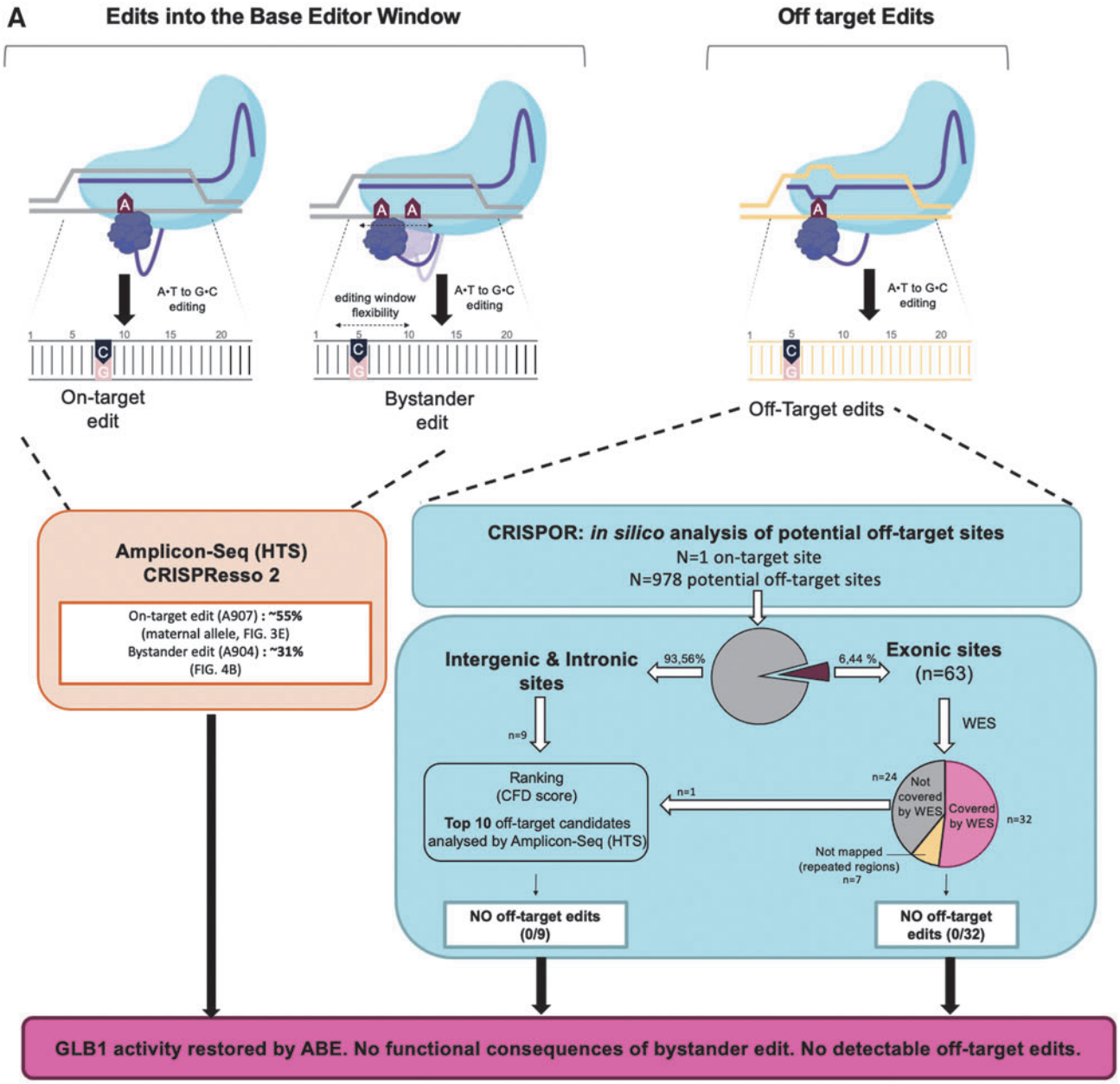
A
Edits into the Base Editor Window
Off target Edits
A•T to G•C editing
editing window flexibility
On-target edit
Bystander edit
Off-Target edits
Amplicon-Seq (HTS)
CRISPResso 2
On-target edit (A907) : ~55%
(maternal allele, FIG. 3E)
Bystander edit (A904) : ~31%
(FIG. 4B)
CRISPOR: in silico analysis of potential off-target sites
N=1 on-target site
N=978 potential off-target sites
Intergenic & Intronic sites
93,56%
6,44 %
Exonic sites
(n=63)
n=9
WES
Ranking
(CFD score)
Top 10 off-target candidates analysed by Amplicon-Seq (HTS)
n=1
n=24
Not covered by WES
Covered by WES
n=32
Not mapped (repeated regions)
n=7
NO off-target edits (0/9)
NO off-target edits (0/32)
GLB1 activity restored by ABE. No functional consequences of bystander edit. No detectable off-target edits.

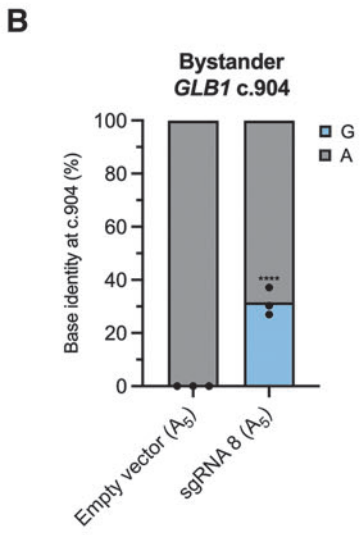
B
Bystander
GLB1 c.904
Base identity at c.904 (%)
G
A
Empty vector (A5)
sgRNA 8 (A5)

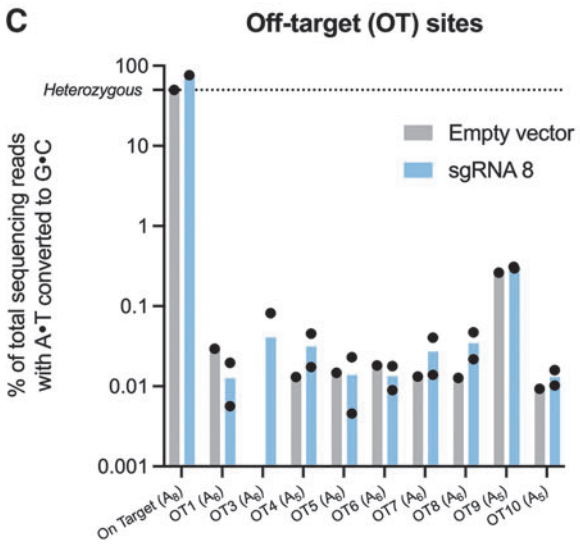
C
Off-target (OT) sites
Heterozygous
Empty vector
sgRNA 8
% of total sequencing reads with A•T converted to G•C
On Target (A6)
OT1 (A6)
OT3 (A6)
OT4 (A6)
OT5 (A6)
OT6 (A6)
OT7 (A6)
OT8 (A6)
OT9 (A6)
OT10 (A6)

viral vectors in gene therapy raises the possibility of rare vector integration into the genome of patient's cells, which may promote oncogenesis.[3,8,46] Recently, another strategy has been published with Virus-like particles (VLPs) efficiently ''infecting cells'' without carrying viral genetic material. So the safety and efficiency of VLPs render them promising for gene editing approaches, including *in vivo*.[7,47]

Limit of the study

To treat GM1 gangliosidosis, a classical gene restoration strategy (rescue) is promising due to the lack of hotspot mutations for this lysosome storage disease (Fig. 1), and currently in clinical trials. In other words, the same vector might be useful for all these patients. This rescue approach has been successful in mice and cats using AAV vectors.[21,24,26–29] It is tempting to postulate that the survival of GM1 patients treated by gene restoration might be long. Thus, the potential drawback of this approach might be a possible decrease of β-gal protein expression level in long term because the AAV vectors are not conceived to integrate the *GLB1* sequence into the patient genome. This limitation has also been discussed in a recent publication.[26]

On the other hand, gene editing is an alternative strategy to cure GM1 gangliosidosis, by correcting the root cause of disease and probably avoiding repetitive adeno-associated virus injections. However, the main limitation of gene editing to treat such pathologies without hotspots is the need to design and evaluate the efficiency and specificity of a sgRNA per patient. Despite these hurdles, efforts to develop more therapeutics to treat rare and ultra-rare diseases are currently increasing in nonprofit biotechnology companies and academic laboratories.

In August 2022, Cure Rare Disease achieved FDA approval for the first-in-human IND to treat a rare mutation causing Duchenne muscular dystrophy using a tailor-made CRISPR approach. The drug, named CRD-TMH-001, treats promoter and exon 1 mutations on the dystrophin gene in muscle. The therapeutic will upregulate an alternate form (isoform) of the dystrophin protein using CRISPR transactivator with the goal of stabilizing, or potentially reversing, symptom progression of Duchenne muscular dystrophy. The dosing of the drug will occur imminently at University of Massachusetts Chan Medical School (one-time administration).

Nowadays, traditional gene addition therapy seems more adapted for these kinds of diseases. However, the situation is changing rapidly. To date, gene editing is well suited to correct autosomal dominant or dominant-negative pathogenic variants[26,48,49] and diseases associated with frequent variants. Three BE treatments are starting a clinical evaluation in humans: VERVE-101 (NCT05398029, Verve Therapeutics) for heterozygous familial hypercholesterolemia (PCSK9 gene), BEAM-101 (NCT05456880, Beam Therapeutics) for Sickle Cell Disease (HBB gene), and BE CAR-7 (base-edited T cells, ISRCTN15323014, Medical Research Council United Kingdom) for T cell leukemia.

Off-target edits might restrain the utility of gene editing for human therapy. In this study, by combining WES and amplicon sequencing for the 10 potential off-target sites ranked by CRISPOR, we did not identify off-target edits in our experimental conditions (0/41 sites). It is important to note that off-target editing independent of the DNA-sgRNA pairing has not been investigated in this study. For a deeper DNA off-target identification, unbiased genome wide, empirical approaches (either biochemical or cell culture based) should be more relevant as some sites may be missed by *in silico* off-target prediction programs.[50,51]

In addition, whole genome sequencing and RNA editing by base editor must be analyzed for a clinical application, according to the recent FDA press release (Human Gene Therapy Products Incorporating Human Genome Editing). In this study, we performed a proof-of-concept study using patient-derived fibroblasts. Additional experiments are needed to replicate these results in cells derived from additional patients and/or new GM1 gangliosidosis models. Indeed, several GM1 gangliosidosis animal models are available, but the *GLB1* genetic modifications carried by these animals are not compatible for a correction by BE.[24,26–29] In the future, a GM1 animal model carrying such compatible mutation might be developed to evaluate *in vivo* the gene editing efficiency/feasibility as already done for progeria.[8]

Conclusion

GM1 gangliosidosis is a rare autosomal recessive disorder estimated to occur in 1 in 100,000 to 200,000 newborns. In this study, we showed that 56% of the pathogenic mutations in *GLB1* gene might be targeted by the BE (ABE+CBE) and 100% by the PE. Importantly, only one pathogenic allele needs to be corrected to cure the disease. Moreover, we demonstrated the efficiency and the safety of ABE in patient-derived fibroblasts in accordance with other BE studies.[8,18] In conclusion, our study strongly suggests that gene editing might be an alternative strategy to cure GM1 gangliosidosis immediately after birth to limit irreversible damage.

Acknowledgments

First, the authors would like to thank the family (parents and son) for their kind support.

We would like to thank their collaborators for helpful advices, protocols, and vectors: Pr. C. Bendavid, Dr. C. Moreau, Pr. D.R. Liu (vectors), Pr. B. Kleinstiver [pCMV-T7-ABEmax(7.10)-SpRY-P2A-EGFP (RTW5025)], the Biosit platforms, especially Dr. P. Gripon for BSL3 and L. Deleurme and A. Aimé for FACS analysis, the CRISP'edit platform (Bordeaux), especially Dr. B. Turcq and Dr. V. Prouzet-Mauleon, the head of the Inserm research unit Dr. E. Chevet, the technicians from the Cell Biology service CHU Rennes, and Pr. E. Tucker and Dr. A. Matvere for critical reading of this article.

Authors' Contributions

D.L.: conceptualization, data curation, formal analysis, investigation, visualization, validation, writing—original draft, and writing—review and editing.

L.G.: data curation, investigation, and writing—review and editing.

S.J.: data curation, formal analysis, investigation, project administration, and writing—review and editing.

B.N.: data curation, formal analysis, validation, software, and writing—review and editing.

L.C.: investigation and writing—review and editing.

L.D.: resources and writing—review and editing.

C.D.: data curation, investigation, resources, and writing—review and editing.

A.E.: data curation, investigation, and writing—review and editing.

T.L.: investigation, resources, and writing—review and editing.

R.F.: investigation, resources, writing—review and editing.

S.D.: data curation, investigation, and writing—review and editing.

X.G.: investigation and writing—review and editing.

L.A.E.: investigation and writing—review and editing.

E.L.: data curation, investigation, and writing—review and editing.

F.M.: project administration and writing—review and editing.

M.-A.B.-R.: project administration and writing—review and editing.

S.O.: resources and project administration.

D.G.: conceptualization, data curation, formal analysis, investigation, visualization, validation, writing—original draft, writing—review and editing, and project administration.

Author Disclosure Statement

No competing financial interests exist.

Funding Information

The authors would like to thank their sponsors: ANR ANR-21-CE18-0020, Cancéropôle Grand-Ouest, AVIESAN Plan Cancer, Ministère de l'enseignement Supérieur, de la Recherche et de l'Innovation (PhD fellowship), Grants to LAE from the Swedish Research Council (VR; Grant No. 2019-3684) and the Swedish Cancer Foundation (Grant No. 21-1447-Pj), and allocation of computing time provided by the Swedish National Infrastructure for Computing at supercomputing center C3SE and NSC, in part, funded by the Swedish Research Council through grant agreement no. 2018-05973. XG is grateful to the Fondation ARC pour la recherche sur le cancer for his postdoctoral fellowship (PDF20191209830).

Supplementary Material

Supplementary Figure S1
Supplementary Figure S2
Supplementary Figure S3
Supplementary Figure S4
Supplementary Table S1
Supplementary Table S2
Supplementary Table S3
Supplementary Table S4
Supplementary Table S5

References

1. Saha K, Sontheimer EJ, Brooks PJ, et al. The NIH somatic cell genome editing program. Nature 2021;592(7853):195–204; doi: 10.1038/s41586-021-03191-1
2. Doudna JA. The promise and challenge of therapeutic genome editing. Nature 2020;578(7794):229–236; doi: 10.1038/s41586-020-1978-5
3. Anzalone AV, Koblan LW, Liu DR. Genome editing with CRISPR-Cas nucleases, base editors, transposases and prime editors. Nat Biotechnol 2020;38(7):824–844; doi: 10.1038/s41587-020-0561-9
4. Newby GA, Liu DR. In vivo somatic cell base editing and prime editing. Mol Ther 2021;29(11):3107–3124; doi: 10.1016/j.ymthe.2021.09.002
5. Newby GA, Yen JS, Woodard KJ, et al. Base editing of haematopoietic stem cells rescues sickle cell disease in mice. Nature 2021;595(7866):295–302; doi: 10.1038/s41586-021-03609-w
6. Krishnamurthy S, Traore S, Cooney AL, et al. Functional correction of CFTR mutations in human airway epithelial cells using adenine base editors. Nucleic Acids Res 2021;49(18):10558–10572; doi: 10.1093/nar/gkab788
7. Banskota S, Raguram A, Suh S, et al. Engineered virus-like particles for efficient in vivo delivery of therapeutic proteins. Cell 2022;185(2):250–265.e16; doi: 10.1016/j.cell.2021.12.021
8. Koblan LW, Erdos MR, Wilson C, et al. In vivo base editing rescues Hutchinson-Gilford progeria syndrome in mice. Nature 2021;589(7843):608–614; doi: 10.1038/s41586-020-03086-7
9. Musunuru K, Chadwick AC, Mizoguchi T, et al. In vivo CRISPR base editing of PCSK9 durably lowers cholesterol in primates. Nature 2021;593(7859):429–434; doi: 10.1038/s41586-021-03534-y
10. Kleinstiver BP, Pattanayak V, Prew MS, et al. High-fidelity CRISPR-Cas9 nucleases with no detectable genome-wide off-target effects. Nature 2016;529(7587):490–495; doi: 10.1038/nature16526
11. Boutin J, Cappellen D, Rosier J, et al. ON-target adverse events of CRISPR-Cas9 nuclease: More chaotic than expected. CRISPR J 2022;5(1):19–30; doi: 10.1089/crispr.2021.0120
12. Gaudelli NM, Lam DK, Rees HA, et al. Directed evolution of adenine base editors with increased activity and therapeutic application. Nat Biotechnol 2020;38(7):892–900; doi: 10.1038/s41587-020-0491-6
13. Rees HA, Minella AC, Burnett CA, et al. CRISPR-derived genome editing therapies: Progress from bench to bedside. Mol Ther 2021;29(11):3125–3139; doi: 10.1016/j.ymthe.2021.09.027

14. Komor AC, Kim YB, Packer MS, et al. Programmable editing of a target base in genomic DNA without double-stranded DNA cleavage. Nature 2016;533(7603):420–424; doi: 10.1038/nature17946
15. Gaudelli NM, Komor AC, Rees HA, et al. Programmable base editing of A•T to G•C in genomic DNA without DNA cleavage. Nature 2017;551(7681):464–471; doi: 10.1038/nature24644
16. Tan J, Zhang F, Karcher D, et al. Engineering of high-precision base editors for site-specific single nucleotide replacement. Nat Commun 2019;10(1):439; doi: 10.1038/s41467-018-08034-8
17. Jia K, Cui Y ru, Huang S, et al. Phage peptides mediate precision base editing with focused targeting window. Nat Commun 2022;13(1):1662; doi: 10.1038/s41467-022-29365-7
18. Rees HA, Komor AC, Yeh W-H, et al. Improving the DNA specificity and applicability of base editing through protein engineering and protein delivery. Nat Commun 2017;8:15790; doi: 10.1038/ncomms15790
19. Walton RT, Christie KA, Whittaker MN, et al. Unconstrained genome targeting with near-PAMless engineered CRISPR-Cas9 variants. Science 2020;368(6488):290–296; doi: 10.1126/science.aba8853
20. Huang TP, Newby GA, Liu DR. Precision genome editing using cytosine and adenine base editors in mammalian cells. Nat Protoc 2021;16(2):1089–1128; doi: 10.1038/s41596-020-00450-9
21. Nicoli E-R, Annunziata I, d'Azzo A, et al. GM1 gangliosidosis—A mini-review. Front Genet 2021;12:734878; doi: 10.3389/fgene.2021.734878
22. Lang FM, Korner P, Harnett M, et al. The natural history of type 1 infantile GM1 gangliosidosis: A literature-based meta-analysis. Mol Genet Metab 2020;129(3):228–235; doi: 10.1016/j.ymgme.2019.12.012
23. McCurdy VJ, Johnson AK, Gray-Edwards HL, et al. Sustained normalization of neurological disease after intracranial gene therapy in a feline model. Sci Transl Med 2014;6(231):231ra48; doi: 10.1126/scitranslmed.3007733
24. Hinderer C, Nosratbakhsh B, Katz N, et al. A single injection of an optimized adeno-associated viral vector into cerebrospinal fluid corrects neurological disease in a murine model of GM1 gangliosidosis. Hum Gene Ther 2020;31(21–22):1169–1177; doi: 10.1089/hum.2018.206
25. Levy JM, Yeh W-H, Pendse N, et al. Cytosine and adenine base editing of the brain, liver, retina, heart and skeletal muscle of mice via adeno-associated viruses. Nat Biomed Eng 2020;4(1):97–110; doi: 10.1038/s41551-019-0501-5
26. Gross AL, Gray-Edwards HL, Bebout CN, et al. Intravenous delivery of adeno-associated viral gene therapy in feline GM1 gangliosidosis. Brain 2022;145(2):655–669; doi: 10.1093/brain/awab309
27. Baek RC, Boekman MLD, Leroy SG, et al. AAV-mediated gene delivery in adult GM1-gangliosidosis mice corrects lysosomal storage in CNS and improves survival. PLoS One 2010;5(10):e13468; doi: 10.1371/journal.pone.0013468
28. Weismann CM, Ferreira J, Keeler AM, et al. Systemic AAV9 gene transfer in adult GM1 gangliosidosis mice reduces lysosomal storage in CNS and extends lifespan. Hum Mol Genet 2015;24(15):4353–4364; doi: 10.1093/hmg/ddv168
29. Broekman MLD, Baek RC, Comer LA, et al. Complete correction of enzymatic deficiency and neurochemistry in the GM1-gangliosidosis mouse brain by neonatal adeno-associated virus-mediated gene delivery. Mol Ther 2007;15(1):30–37; doi: 10.1038/sj.mt.6300004
30. Buchlis G, Podsakoff GM, Radu A, et al. Factor IX expression in skeletal muscle of a severe hemophilia B patient 10 years after AAV-mediated gene transfer. Blood 2012;119(13):3038–3041; doi: 10.1182/blood-2011-09-382317
31. Muhuri M, Levy DI, Schulz M, et al. Durability of transgene expression after RAAV gene therapy. Mol Ther 2022;30(4):1364–1380; doi: 10.1016/j.ymthe.2022.03.004
32. Mouden C, Dubourg C, Carré W, et al. Complex mode of inheritance in holoprosencephaly revealed by whole exome sequencing. Clin Genet 2016;89(6):659–668; doi: 10.1111/cge.12722
33. Ho MW, O'Brien JS. Hurler's syndrome: Deficiency of a specific beta galactosidase isoenzyme. Science 1969;165(3893):611–613; doi: 10.1126/science.165.3893.611
34. Kleinstiver BP, Prew MS, Tsai SQ, et al. Engineered CRISPR-Cas9 nucleases with altered PAM specificities. Nature 2015;523(7561):481–485; doi: 10.1038/nature14592
35. Haeussler M, Schönig K, Eckert H, et al. Evaluation of off-target and on-target scoring algorithms and integration into the guide RNA selection tool CRISPOR. Genome Biol 2016;17(1):148; doi: 10.1186/s13059-016-1012-2
36. Doench JG, Fusi N, Sullender M, et al. Optimized sgRNA design to maximize activity and minimize off-target effects of CRISPR-Cas9. Nat Biotechnol 2016;34(2):184–191; doi: 10.1038/nbt.3437
37. Clement K, Rees H, Canver MC, et al. CRISPResso2 provides accurate and rapid genome editing sequence analysis. Nat Biotechnol 2019;37(3):224–226; doi: 10.1038/s41587-019-0032-3
38. Bowers KJ, Chow E, Xu H, et al. Scalable Algorithms for Molecular Dynamics Simulations on Commodity Clusters. In: Proceedings of the 2006 ACM/IEEE Conference on Supercomputing, SC'06; Association for Computing Machinery: New York, NY, United States: 2006; doi: 10.1109/SC.2006.54
39. Lu C, Wu C, Ghoreishi D, et al. OPLS4: Improving force field accuracy on challenging regimes of chemical space. J Chem Theory Comput 2021;17(7):4291–4300; doi: 10.1021/acs.jctc.1c00302
40. Jorgensen WL, Chandrasekhar J, Madura JD, et al. Comparison of simple potential functions for simulating liquid water. J Chem Phys 1983;79(2):445869; doi: 10.1063/1.445869
41. Morrone A, Morreau H, Zhou XY, et al. Insertion of a T next to the donor splice site of intron 1 causes aberrantly spliced mRNA in a case of infantile GM1-gangliosidosis. Hum Mutat 1994;3(2):112–120; doi: 10.1002/humu.1380030205
42. Anzalone AV, Randolph PB, Davis JR, et al. Search-and-replace genome editing without double-strand breaks or donor DNA. Nature 2019;576(7785):149–157; doi: 10.1038/s41586-019-1711-4
43. Finkel RS, Chiriboga CA, Vajsar J, et al. Treatment of infantile-onset spinal muscular atrophy with nusinersen: A phase 2, open-label, dose-escalation study. Lancet 2016;388(10063):3017–3026; doi: 10.1016/S0140-6736(16)31408-8
44. Akcakaya P, Bobbin ML, Guo JA, et al. In vivo CRISPR editing with no detectable genome-wide off-target mutations. Nature 2018;561(7723):416–419; doi: 10.1038/s41586-018-0500-9
45. Yeh W-H, Chiang H, Rees HA, et al. In vivo base editing of post-mitotic sensory cells. Nat Commun 2018;9(1):2184; doi: 10.1038/s41467-018-04580-3
46. Chandler RJ, Sands MS, Venditti CP. Recombinant adeno-associated viral integration and genotoxicity: Insights from animal models. Hum Gene Ther 2017;28(4):314–322; doi: 10.1089/hum.2017.009
47. Mangeot PE, Risson V, Fusil F, et al. Genome editing in primary cells and in vivo using viral-derived Nanoblades loaded with Cas9-sgRNA ribonucleoproteins. Nat Commun 2019;10(1):45; doi: 10.1038/s41467-018-07845-z
48. Diakatou M, Manes G, Bocquet B, et al. Genome editing as a treatment for the most prevalent causative genes of autosomal dominant retinitis pigmentosa. Int J Mol Sci 2019;20(10):2542; doi: 10.3390/ijms20102542
49. Bakondi B, Lv W, Lu B, et al. In vivo CRISPR/Cas9 gene editing corrects retinal dystrophy in the S334ter-3 rat model of autosomal dominant retinitis pigmentosa. Mol Ther 2016;24(3):556–563; doi: 10.1038/mt.2015.220
50. Kim D, Kang BC, Kim JS. Identifying genome-wide off-target sites of CRISPR RNA–guided nucleases and deaminases with Digenome-seq. Nat Protoc 2021;16(2):1170–1192; doi: 10.1038/s41596-020-00453-6
51. Lei Z, Meng H, Lv Z, et al. Detect-seq reveals out-of-protospacer editing and target-strand editing by cytosine base editors. Nat Methods 2021;18(6):643–651; doi: 10.1038/s41592-021-01172-w

Received: April 19, 2022
Accepted: November 19, 2022
Online Publication Date: January 9, 2023